WILEY | Hindawi

Research Article

Team Recruitment of Collaborative Crowdsensing under Joint Constraints of Willingness and Trust

Nianyun Song [ID],[1,2] **Dianjie Lu** [ID],[1,2,3] **Chunyu Hu**,[2,4] **Weizhi Xu**,[1,2,3] **and Guijuan Zhang** [ID][1,2,3]

[1]*School of Information Science and Engineering, Shandong Normal University, Jinan 250358, China*
[2]*Shandong Provincial Key Laboratory for Novel Distributed Computer Software Technology, Jinan 250358, China*
[3]*State Key Laboratory of High-End Server & Storage Technology, Organization, Jinan 250358, China*
[4]*School of Computer Science and Technology (Shandong Academy of Sciences), Qilu University of Technology, Jinan 250358, China*

Correspondence should be addressed to Dianjie Lu; ludianjie@sdnu.edu.cn and Guijuan Zhang; zhangguijuan@sdnu.edu.cn

Collaborative crowdsensing (CCS) requires the recruited team to collaborate closely to complete sensing tasks with high quality of service (QoS). The team recruitment of CCS is mainly influenced by the subjective willingness of participants and the objective trust evaluation of the sensing platform; that is, the higher the subjective mutual willingness to work together and the objective mutual trust among participants, the more efficiency with which the CCS tasks will be achieved. However, the existing research lacks comprehensive consideration of mutual willingness and mutual trust among recruited participants. This results in poor QoS. To address this problem, we propose a novel team recruitment method for CCS that jointly considers the willingness and trust to recruit optimal teams. First, we build a graph convolutional network-based willingness-trust network (GCN-WTN) model for CCS to obtain mutual willingness and trust among participants more accurately. Second, we propose a willingness and trust-based team recruitment (WT-TR) method to recruit the optimal teams for CCS. This method introduces the consensus and similarity constraints into the willingness and trust networks to better meet the collaboration needs of CCS. Finally, we implement a recruitment simulation platform for CCS to simulate the team recruitment process and validate the effectiveness of our proposed method. The experimental results show that the teams recruited by the proposed method can significantly improve QoS for CCS.

1. Introduction

With the rapid development of intelligent devices such as mobile phones, crowdsensing provides a new opportunity for information collection [1]. However, as sensing tasks become increasingly complex and large-scale, crowdsensing often requires interaction and collaboration among participants. This type of sensing is called collaborative crowdsensing (CCS). For instance, crowd evacuation path planning requires the collection, uploading, forwarding, and fusing of information from the crowd at various times and locations [2]. Such a task is difficult to complete for a single individual. Therefore, recruiting optimal teams, so that members of the same team can collaborate and complete

sensing tasks with higher quality of service (QoS), is a challenging problem for CCS.

Participant recruitment plays a crucial role in ensuring the quality of CCS tasks' fulfillment. We can divide crowdsensing participant recruitment into two categories: individual recruitment and team recruitment. Individual recruitment schemes focus on selecting individuals based on evaluation metrics such as dynamic trust, as proposed by Gao et al. [3], or assessing their social influence, as proposed by Wang et al. [4]. These schemes work well for tasks that require low collaboration, such as image tagging and photo collection [5], where the quality of data mainly depends on individual effort. However, such schemes may not be effective for CCS scenarios, where the need for teamwork has

been proposed [6, 7]. Team recruitment involves selecting participants based on their professional knowledge [8], personality traits [9], and social networks [10, 11]. Azzam et al. [12] argued that a group qualifies to perform a task if they successfully cover the task area and are evenly distributed. However, the current recruitment methods are not suitable for CCS team recruitment since they fail to consider the willingness and trust among participants, which can lead to ineffective collaboration and reduce the QoS of CCS. There are indeed many factors that affect team recruitment, but ensuring effective cooperation among participants within the same team is crucial for successful CCS.

An effective team is not a random group but a team with good cooperation abilities to achieve a common goal. The recruitment of optimal teams for CCS is influenced by both subjective and objective factors. Inspired by Barnard's organization theory [13], it is necessary to consider the subjective willingness of participants to cooperate since CCS is a "human-centered" activity. Neglecting the subjective willingness of participants may lead to poor CCS behaviors, such as ineffective execution, withdrawal, or even refusal to cooperate. Lencioni [14] identified a lack of trust among team members as one of the five dysfunctions of a team. This is one of the important characteristics that distinguish effective teams. With the increasing diversity of CCS environments, mutual trust is becoming an essential factor in participants' behavior decisions [15, 16]. Therefore, it is necessary to consider the objective mutual trust among team members, which can ensure successful collaboration by reducing risks and uncertainties of working together [17, 18]. Having a high level of mutual trust among participants is an objective factor that the platform expects from the recruited teams.

To address this problem, we propose a novel team recruitment method for CCS that jointly considers the willingness and trust to recruit the optimal teams so that they can collaborate mutually to complete the sensing tasks with higher QoS. The framework of the proposed method is presented in Figure 1. It includes two modules: (1) modeling of the willingness network and trust network for CCS and (2) willingness and trust-based team recruitment (WT-TR). In the first module, we build a graph convolutional network-based willingness-trust network (GCN-WTN) model for CCS to obtain mutual willingness and trust among participants more accurately. The model uses graph convolutional networks (GCNs) to capture the mutuality of willingness and trust. In the second module, we introduce consensus and similarity constraints into the willingness and trust networks built above to better meet the collaboration needs of CCS. Then, we transform the CCS team recruitment process into dual-view spectral clustering to obtain the optimal teams. Finally, we implement a recruitment simulation platform for CCS to simulate the team recruitment process and validate the effectiveness of our proposed method. To the best of our knowledge, this is the first method that jointly considers willingness and trust with the consensus and similarity constraints to recruit the optimal teams for CCS. The main contributions of this paper are as follows:

(1) We build the GCN-WTN model for CCS to obtain mutual willingness and trust among participants more accurately.

(2) We propose the WT-TR method to recruit the optimal teams for CCS. This method introduces the consensus and similarity constraints into the willingness and trust networks to better meet the collaboration needs of CCS.

(3) We implement a recruitment simulation platform for CCS to simulate the team recruitment process and validate the effectiveness of our proposed method.

The remainder of this article is organized as follows: Section 2 reviews the related work. Section 3 describes the model of the willingness network and trust network for CCS. Section 4 formulates the WT-TR method in detail. Section 5 presents the recruitment simulation platform for CCS and the analysis of experimental results, and Section 6 consists of the conclusions and future work.

2. Related Work

The success of crowdsensing services is entirely dependent on the sensing behavior of the recruited participants from the users' point of view. Hence, the primary focus of research in crowdsensing is participant recruitment, i.e., selecting the right participants to perform the sensing task effectively. Based on the selection criteria, relevant research work is divided into individual recruitment and team recruitment.

2.1. Individual Recruitment of Crowdsensing. Zhang et al. [19] proposed a recruitment algorithm that aimed to cover all target sensing areas in a cost-effective manner by using a greedy approach. Hu et al. [20] proposed a reinforcement learning-based recruitment framework that could accurately predict the position of participants by gradually accumulating the movement trajectories of individual participants and selecting the most appropriate candidates. Gao et al. [21] introduced a learning-based credible participant recruitment strategy (LC-PRS) that aimed to maximize the benefits of both the platform and participants. Wang et al. [22] proposed a personalized and task-oriented worker recruitment mechanism that accurately predicted workers' preferences for tasks by analyzing their implicit feedback and then recruiting the most suitable workers. Ota et al. [23] introduced a novel incentive mechanism called quality and usability of information (QUOIN) that aimed to increase participants' willingness to participate. QUOIN used the Stackelberg game model to ensure that each participant could earn a satisfactory profit. Jin et al. [24] developed a payment mechanism called Theseus that considered the strategic behavior of workers. Theseus aimed to motivate workers to provide high-quality data and was combined with a truth discovery algorithm. Lv et al. [25] proposed a privacy-preserving truth discovery mechanism called efficient slicing-based privacy-preserving truth discovery (ESPPTD)
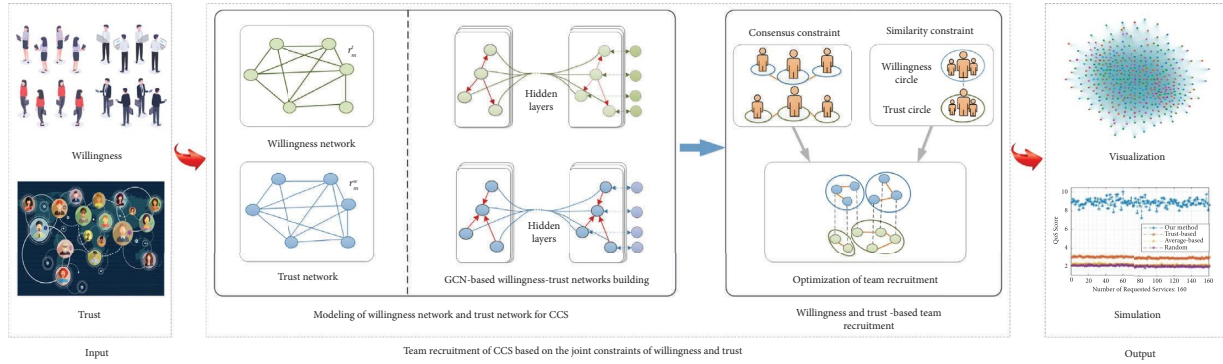
FIGURE 1: The framework of our method.

to increase participants' willingness to participate from a privacy perspective. Restuccia et al. [26] proposed a dynamic trust-based framework that used a limited number of high-trust participants to establish credibility in a secure manner, thereby preventing security attacks of malicious participants. Gao et al. [3] also proposed a similar framework to recruit credible participants. Their framework calculated the combined trust of participants by considering direct trust, feedback trust, and incentive functions.

In most of the abovementioned recruitment methods, individual participants are recruited based on evaluation metrics such as spatial coverage, cost, personal preference, individual willingness, and individual trust. These methods assume that participants can complete the task alone without any interaction with one another. However, with the increasing complexity of crowdsensing tasks, there is a growing need for collaboration and interaction among participants.

2.2. Team Recruitment of Crowdsensing. In recent years, researchers have increasingly recognized the value of team recruitment for crowdsensing and conducted extensive research in this area [7, 27]. For instance, Hamrouni et al. [28] proposed and discussed two team recruitment strategies: platform-based and leader-based. By considering participants' professional knowledge and social connections, a group of individuals were recruited to work together on complex tasks within a budget. Jiang and Matsubara [8] focused on dividing complex tasks into simpler subtask streams and assigning these subtasks to workers for completion. Azzam et al. [29] designed a group recruitment system based on stability, allowing the dynamic addition and deletion of participants to achieve the expected sensing results. However, this system did not consider the credibility of participants. Wang et al. [30] focused more on the platform budget and divided participants into two groups to cope with the recruitment of different budgets. On the other hand, Zhu et al. [31] recognized the importance of group role assignment (GRA) in building teams and combined GRA with the E-CARGO model to solve many collaboration problems, such as GRA considering collaboration and conflict factors [32], GRA considering the busyness of subjects [33], and group

multirole assignment (GMRA) [34]. However, their model did not consider willingness and trust relationships among participants. Cheng and Xiao [35] presented a location-based task assignment problem, where the platform assigned complex tasks that required collaboration among multiple participants. However, their study only focused on the assignment of tasks and scheduling.

CCS differs from traditional crowdsensing in that successful task completion requires a greater focus on team members' ability to interact and collaborate closely. CCS team recruitment is affected by objective and subjective factors, such as willingness and trust. Participants may refuse to participate together in the absence of mutual willingness to work together, and the team cooperation platform will collapse without considering the mutual trust among participants. However, the above work does not take into account the mutual willingness and trust relationship among participants simultaneously. This could prevent the participants of the same team from cooperating closely, ultimately decreasing the QoS of CCS.

In this paper, we use the team recruitment scheme, which jointly considers the willingness and trust to recruit the optimal teams to improve the QoS for CCS.

3. Modeling of the Willingness Network and Trust Network for CCS

To recruit teams that can work collaboratively, the subjective willingness to work together and the objective mutual trust among participants are two key factors that must be considered jointly. To facilitate the study of the impact of these two factors on CCS, we construct the model of the willingness network and trust network.

3.1. Willingness Network and Trust Network. We introduce the following definitions to describe the willingness and trust networks.

Definition 1 (willingness network). The willingness network can be modeled by an undirected graph $G_m^w = (U^w, E_m^w, \mathbf{R}_m^w)$, where $U^w = \{1, \cdots, N\}$ is the set of participants, N is the number of participants, E_m^w is the set of edges representing the mutual willingness relationships to work together

between participants, and $\mathbf{R}_m^w$ is the weighted adjacency matrix, the values of which represent the willingness ratings between participants.

If participants i and j are involved in the same task, an edge $e_m^w(i,j) \in E_m^w$ is created between them in the willingness network. A higher weight is assigned to the corresponding edge to indicate a stronger willingness rating between participants i and j. This weight reflects their frequency of working on the same task and their positive evaluation of each other.

Definition 2 (trust network). The trust network can be modeled by an undirected graph $G_m^t = (U^t, E_m^t, \mathbf{R}_m^t)$, where $U^t = \{1, \ldots, N\}$ is the set of participants, N is the number of participants, E_m^t is the set of the mutual trust relationship between participants, and $\mathbf{R}_m^t$ is the weighted adjacency matrix, the values of which represent the trust ratings between participants. Each trust relationship $e_m^t(i,j) \in E_m^t$ is associated with a rating $r_m^t(i,j) \in \mathbf{R}_m^t$, which indicates the degree of mutual trust between the participant i and the participant j.

3.2. GCN-WTN Building.

Without loss of generality, we assume that some willingness and trust relationships can be obtained. In reality, willingness and trust relationships are usually directional and sparse. Traditional work considers the propagation and asymmetry of willingness and trust between participants [36] but lacks research on mutuality, which can reduce the QoS of CCS. GCNs have been proven to learn well about graphical data and have made fresh progress on problems such as node-link prediction [37, 38]. In this subsection, we use GCNs to build willingness and trust networks.

The known willingness relationship is expressed as a directed network $G^w = (U^w, E^w, \mathbf{R}^w)$, where any vertices $i, j \in U^w$ represent participants, $e^w(i,j) \in E^w$ is the known willingness relationship, and $r^w(i,j) \in \mathbf{R}^w$ represents the corresponding willingness rating. Similarly, we use the directed network $G^t = (U^t, E^t, \mathbf{R}^t)$ to represent the known directed trust relationship. The ratings of directed willingness and trust relationships are affected by many factors. For example, the level of directed trust can be calculated based on social trust [39] between participants, and the level of directed willingness can be calculated based on historical records of participants. Additionally, an alternative way to calculate the level of cooperation willingness among participants is based on electroencephalography signals [40]. It is worth noting that the specific rating calculation is not the focus of this paper.

Figure 2 shows the structure of the GCN-WTN building. It consists of two components: (1) a willingness/trust convolution layer and (2) a mutual willingness/trust relationship prediction layer. The input is a directed willingness/trust network, and the output is the willingness/trust network with a mutual willingness/trust relationship. In the willingness/trust convolution layer, participant embeddings are initialized to facilitate GCN learning. Then, we consider the higher order in-neighbors and out-neighbors of each participant to learn the rules of willingness/trust propagation and aggregation. In the mutual willingness/trust relationship prediction layer, we concatenate the embedded vectors of each participant pair to predict the willingness/trust relationship. Then, we convert the predicted asymmetric willingness/trust into mutual willingness/trust to obtain the mutual willingness/trust relationship between participant pairs. The entire model is trained end to end. After training, a convolutional network structure and a vector embedding representation of the participants are obtained.

3.2.1. Willingness/Trust Convolution Layer.

To facilitate the learning of GCNs, we initialize a D-dimension vector embedding $\mathbf{x}$ for each participant and optimize it in an end-to-end fashion. In the following sections, we use the terms nodes and participants interchangeably. Moreover, for the sake of uniform introduction, we do not distinguish the superscripts w and t in G^w and G^t.

To better capture the asymmetry of willingness/trust, we divide the neighbors of each node into two groups: in-neighbors and out-neighbors. An example of in-neighbors and out-neighbors is shown in Figure 3. The in-neighbors' interactions with the node i are the degrees of willingness/trust from other participants to the node i. Conversely, the out-neighbors' interactions of the node i are the degrees of willingness/trust of the node i towards other participants.

(1) In-Neighbor and Out-Neighbor Feature Propagation. To obtain the features of in-neighbors and out-neighbors of each node, we consider the influence of their direct and indirect neighbors. As shown in Figure 3(a), the in-neighbors' feature of the node i depends on their direct neighbors j and q. The corresponding ratings $r(j,i)$ and $r(q,i)$ provide direct evidence about the degree of willingness/trust of nodes j and q have towards the node i. For the indirect neighbor k of the node i, we can derive the effect of the node k on the node i based on $r(k,j)$ and $r(j,i)$. This provides indirect evidence about the degree of willingness/trust of the node k towards the node i.

To represent the willingness/trust ranking of each type, we encode it using one-hot vector. Next, the ranking $r'(i,j)$ encoded by the one-hot vector is converted into a dense ranking vector embedding as follows:

$$\mathbf{D}_{r'(j,i)} = \mathbf{W}_{(j,i)} \cdot r'(j,i), \tag{1}$$

where $\mathbf{W}_{(j,i)}$ is a trainable transformation matrix. Then, the vector embedding $\mathbf{x}[i]$ of the node i and the associated dense rating vector embedding $\mathbf{D}_{r'(j,i)}$ are concatenated to obtain the willingness/trust representation of the node i to the node j, which is represented as follows:

$$\mathbf{I}(j,i) = \mathbf{x}[i] \otimes \mathbf{D}_{r'(j,i)}. \tag{2}$$

The mean aggregator is used to aggregate the in-neighbors' features of the node i. Thus, we can obtain the in-neighbor feature propagation of the node i, represented as follows:
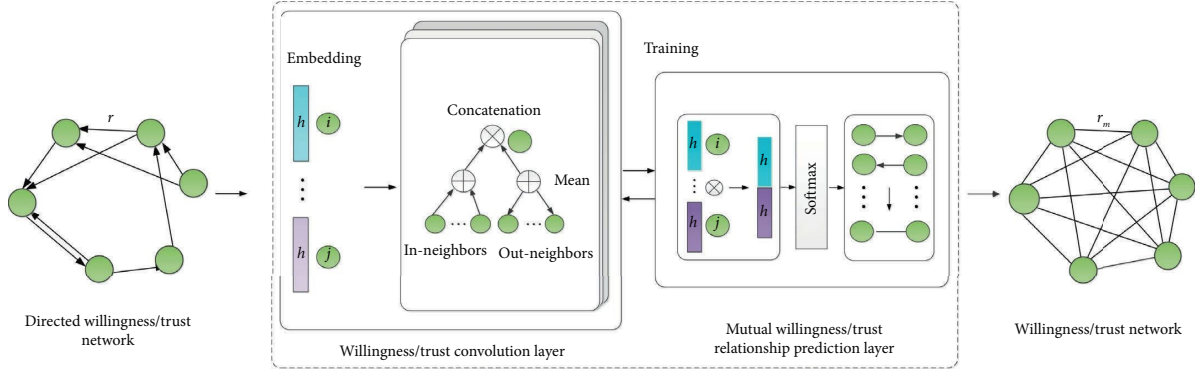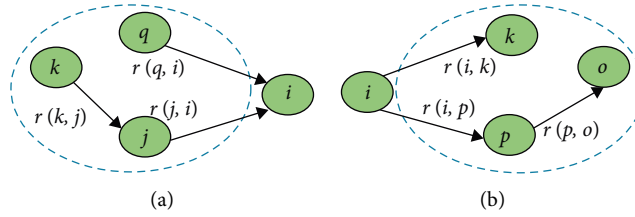
FIGURE 2: GCN-WTN building.

(a) (b)

FIGURE 3: Example of in-neighbors and out-neighbors: (a) The in-neighbors $N_I(i)$ of node i are within the dotted circle. (b) The out-neighbors $N_O(i)$ of node i are within the dotted circle.

$$\mathbf{h}_I[i] = \frac{1}{\left|N_I(i)\right|} \sum_{j \in N_I(i)} \mathbf{I}(j,i). \qquad (3)$$

Similarly, we can obtain the out-neighbor feature propagation of the node i, represented as follows:

$$\mathbf{D}_{r'(i,j)} = \mathbf{W}_{(i,j)} \cdot r'(i,j),$$

$$\mathbf{O}(i,j) = \mathbf{x}[i] \otimes \mathbf{D}_{r'(i,j)}, \qquad (4)$$

$$\mathbf{h}_O[i] = \frac{1}{\left|N_O(i)\right|} \sum_{j \in N_O(i)} \mathbf{O}(i,j).$$

Next, we use a standard fully connected structure to connect the features of the two neighbors of the node i. The final embedded vector of the node i is as follows:

$$\mathbf{h}[i] = \sigma \left(\mathbf{W}_{IO} \cdot \left(\mathbf{h}_I[i] \otimes \mathbf{h}_O[i] \right) + b \right), \qquad (5)$$

where $\mathbf{W}_{IO}$ represents the trainable transformation matrix, b represents the learnable bias, and σ is the nonlinear activation function. Here, we use the softmax function as the activation function.

(2) High-Order Willingness/Trust Feature Propagation. By stacking l convolutional layers, the node i can accept features from its l-hop neighbors. It can be represented as follows:

$$\mathbf{I}^l(j,i) = \mathbf{h}^{l-1}[i] \otimes \mathbf{W}^l_{(j,i)} \cdot r'(j,i),$$

$$\mathbf{O}^l(i,j) = \mathbf{h}^{l-1}[i] \otimes \mathbf{W}^l_{(i,j)} \cdot r'(i,j),$$

$$\mathbf{h}^l_I[i] = \frac{1}{\left|N_I(i)\right|} \sum_{j \in N_I(i)} \mathbf{I}^l(j,i), \qquad (6)$$

$$\mathbf{h}^l_O[i] = \frac{1}{\left|N_O(i)\right|} \sum_{j \in N_O(i)} \mathbf{O}^l(i,j),$$

$$\mathbf{h}^l[i] = \sigma \left(\mathbf{W}^l_{IO} \cdot \left(\mathbf{h}^l_I[i] \otimes \mathbf{h}^l_O[i] \right) + b^l \right),$$

where $\mathbf{h}^0[i] = \mathbf{x}[i]$ is the initialized embedding of the node i. We control its propagation range by adjusting the size of l.

3.2.2. Mutual Willingness/Trust Prediction Layer. To predict the mutual willingness/trust relationship between nodes i and j, the embedding vector representations of nodes i and j are concatenated. By using the softmax function, we can predict the probability of the directed willingness/trust of the node i towards the node j as follows:

$$\widetilde{\mathbf{h}}(i,j) = \sigma \left(\mathbf{W}_p \cdot (\mathbf{h}[i] \otimes \mathbf{h}[j]) \right), \qquad (7)$$

where $\mathbf{W}_p$ denotes the trainable weight matrix defined in the prediction layer and σ is the softmax activation function.

Thus, the directed willingness/trust rating of the node i towards the node j is calculated as follows:

$$\widetilde{r}(i, j) = \underset{r}{\arg\max}(\widetilde{\mathbf{h}}(i, j)). \qquad (8)$$

Due to the asymmetry of willingness/trust, the willingness/trust rating from the node j to the node i is as follows:

$$\widetilde{r}(j, i) = \underset{r}{\arg\max}(\widetilde{\mathbf{h}}(j, i)). \qquad (9)$$

Since mutual collaboration among participants is required for CCS, we convert the asymmetric willingness/trust between each pair of participants into mutual willingness/trust. The lower willingness/trust rating between each pair of nodes is taken as a measure of the mutual willingness/trust relationship, expressed as follows:

$$r_m(i, j) = \min(\widetilde{r}(i, j), \widetilde{r}(j, i)). \qquad (10)$$

To get the best training results, the backpropagation algorithm is used to train the convolutional network structure. Given the proven effectiveness of Adam in updating parameters [41], we choose it as the parameter optimizer. The cross-entropy loss between the predicted and observed true values is the objective function, expressed as follows:

$$\text{Loss} = -\frac{1}{|E|} \sum_{<i,j> \in E} r'(i, j)\log(\widetilde{\mathbf{h}}(i, j)) + \lambda\|\Phi\|_2^2, \qquad (11)$$

where $\left\{\Phi = \left\{\mathbf{W}^l, \mathbf{W}_{IO}^l, b^l\right\}_{l=1}^L, \mathbf{W}_p\right\}$ denotes all trainable parameters and λ is used to control the regularization effect to prevent overfitting.

4. WT-TR

In this section, to better meet the collaboration needs of CCS, we introduce the consensus and similarity constraints into the willingness and trust networks to better jointly consider willingness and trust. Then, we formulate and solve the optimization problem of CCS team recruitment to obtain the optimal teams.

4.1. Consensus Constraint. Let $\text{Team}^w = \{\text{Team}_1^w, \ldots, \text{Team}_C^w\}$ and $\text{Team}^t = \{\text{Team}_1^t, \ldots, \text{Team}_C^t\}$ denote the teams built in the willingness and trust networks, respectively, where C is the number of teams. Team_c^w (Team_c^t) refer to the c th team built in the willingness (trust) network. To facilitate presentation, two team assignment matrices $\mathbf{M}^w = [M^w(i, c)] \in R^{N \times C}$ and $\mathbf{M}^t = [M^t(i, c)] \in R^{N \times C}$ are defined to represent Team^w and Team^t, respectively. The elements in these two matrices are expressed as follows:

$$\begin{cases} M^w(i, c) = \begin{cases} \dfrac{1}{\sqrt{|Team_c^w|}}, if\ i^w \in \text{Team}_c^w, \\ \\ 0, \qquad\qquad \text{otherwise}, \end{cases} \\ \\ M^t(i, c) = \begin{cases} \dfrac{1}{\sqrt{|Team_c^t|}}, if\ i^t \in \text{Team}_c^t, \\ \\ 0, \qquad\qquad \text{otherwise}, \end{cases} \end{cases} \qquad (12)$$

where $|\text{Team}_c^w|$ ($|\text{Team}_c^t|$) represent the number of participants of the c th team in the willingness (trust) network and i^w (i^t) represent the i th participant in the willingness (trust) network.

According to equation (12), we can deduce the orthogonal properties of $\mathbf{M}^w$ and $\mathbf{M}^t$ as follows:

$$\begin{cases} \mathbf{M}^{w^\top}\mathbf{M}^w = \mathbf{I}, \\ \mathbf{M}^{t^\top}\mathbf{M}^t = \mathbf{I}. \end{cases} \qquad (13)$$

Definition 3 (consensus constraint). The consensus constraint is used to ensure that the recruited teams reach a consensus on willingness and trust. We minimize the difference between the team assignment matrices $\mathbf{M}^w$ and $\mathbf{M}^t$ on the willingness network and trust networks to achieve the consensus constraint.

Participants may have different degrees of willingness and trust relationships, which can lead to different team distributions in the willingness and trust networks. To solve this problem, we do not force the teams built in the willingness network and the trust network to be completely equal, that is, $\mathbf{M}^w \neq \mathbf{M}^t$. Instead, inspired by Kumar et al. [42], we minimize equation (14) to achieve the consensus constraint:

$$\text{Con}(\mathbf{M}^w, \mathbf{M}^t) = \left\| \frac{\mathbf{M}^w \mathbf{M}^{w^\top}}{\|\mathbf{M}^w\|_F^2} - \frac{\mathbf{M}^t \mathbf{M}^{t^\top}}{\|\mathbf{M}^t\|_F^2} \right\|_F^2, \qquad (14)$$

where $\|\mathbf{M}^w\|_F^2 = tr(\mathbf{M}^w \mathbf{M}^{w^\top}) = C$ and $\|\mathbf{M}^t\|_F^2 = tr(\mathbf{M}^t \mathbf{M}^{t^\top}) = C$.

4.2. Similarity Constraint. According to the principle of "neighborhood protection" [43], there are similarities in the willingness and trust relationships between participants and their immediate neighbors. Participants with mutual trust are more likely than average to participate in the same sensing tasks together. The willingness of participants to

participate in sensing tasks can in turn strengthen their mutual trust. Thus, the participant behaviors in the two networks of willingness and trust are to some extent compatible, rather than independent.

Definition 4 (similarity constraint).The similarity constraint describes similar interaction contexts of the same participants in different networks.

For the participant i, we select the K-nearest neighbors who have the highest willingness and the highest trust with the participant i in the willingness and trust networks, respectively. Based on these selections, we construct the interaction contexts of the willingness circle and trust circles for the participant i as follows:

$$\begin{cases} W_K\left(i^w\right) = \{i_1^w, \ldots, i_K^w\}, \\ T_K\left(i^t\right) = \{i_1^t, \ldots, i_K^t\}, \end{cases} \tag{15}$$

where i_k^w and i_k^t are the k th nearest neighbors of the i th participant in the willingness and trust networks, respectively. We define two neighbor selection matrices $\mathbf{X}_i^w = [X_i^w(j,k)] \in R^{N \times K}$ and $\mathbf{X}_i^t = [X_i^t(j,k)] \in R^{N \times K}$, where each participant i selects his/her neighbors according to equation (15). The elements of these two matrices are given by

$$\begin{cases} X_i^w(j,k) = \begin{cases} 1, & if\ j = i_k^w \in W_K\left(i^w\right), \\ 0, & \text{otherwise}, \end{cases} \\ X_i^t(j,k) = \begin{cases} 1, & if\ j = i_k^t \in T_K\left(i^t\right), \\ 0, & \text{otherwise}. \end{cases} \end{cases} \tag{16}$$

According to the willingness circle and trust circles of the participant i, the corresponding K distribution vectors of C teams can be selected from $\mathbf{M}^w$ and $\mathbf{M}^t$. Then, we can define the context team assignment matrices $\mathbf{M}_i^w \in R^{K \times C}$ and $\mathbf{M}_i^t \in R^{K \times C}$ for the participant i as follows:

$$\begin{cases} \mathbf{M}_i^w = \mathbf{X}_i^{w\top}\mathbf{M}^w, \\ \mathbf{M}_i^t = \mathbf{X}_i^{t\top}\mathbf{M}^t. \end{cases} \tag{17}$$

Given the K-nearest neighbors and the context team assignment matrices of the participant i, we impose the similarity constraint on the willingness and trust networks. Specifically, we aim to ensure that the distribution of the participant i's K-nearest neighbors is similar in the willingness and trust networks. It is assumed that each team c places similar weights on its K neighbors. Therefore, there should be a sufficiently small difference between $\sum_{k=1}^{K}\mathbf{M}_i^w(k,c)$ and $\sum_{k=1}^{K}\mathbf{M}_i^t(k,c)$. To achieve the similarity constraint for the participant i, we minimize the following formula:

$$\text{Sim}\left(\mathbf{M}_i^w, \mathbf{M}_i^t\right) = \sum_{c=1}^{C}\left(\sum_{k=1}^{K}M_i^w(k,c) - \sum_{k=1}^{K}M_i^t(k,c)\right)^2 = \left\|\left(\mathbf{M}_i^w - \mathbf{M}_i^t\right)^{\top}\mathbf{e}\right\|^2, \tag{18}$$

where $\mathbf{e}$ is a vector of all ones. The similarity constraint for all participants is as follows:

$$\text{Sim}\left(\mathbf{M}^w, \mathbf{M}^t\right) = \sum_{i=1}^{N}\left\|\left(\mathbf{M}_i^w - \mathbf{M}_i^t\right)^{\top}\mathbf{e}\right\|^2. \tag{19}$$

4.3. The Formulation and Solution of CCS Team Recruitment Optimization.

To improve the QoS of CCS, we are committed to recruiting the optimal teams Team = $\{\text{Team}_1, \ldots, \text{Team}_C\}$ by dividing all participants into C teams. Essentially, this is a classification problem, where participants are assigned to teams based on their willingness and trust relationships. In each team, participants have a higher mutual willingness and trust so that they can collaborate more effectively to complete sensing tasks. In the optimization of CCS team recruitment, participants and teams are both parties to team recruitment. The formal definition of the CCS team recruitment optimization problem is as follows.

Definition 5 (CCS team recruitment optimization problem). Given a set of N participants with mutual willingness and trust relationships and C required teams, our goal is to recruit these N participants into C optimal teams Team = $\{\text{Team}_1, \ldots, \text{Team}_C\}$. The teams should satisfy both consensus and similarity constraints on the willingness and trust networks to ensure effective completion of CCS tasks.

Multiview spectral clustering can divide objects into different cohesive clusters by exploring the consensus with multiple views [44, 45]. Hence, to obtain the optimal teams using the willingness network and trust network, we transform the CCS team recruitment process into dual-view spectral clustering. The willingness network can be seen as describing the mutual willingness relationship among participants to participate in sensing tasks together from the willingness view. The trust network can be seen as describing the mutual trust relationship among participants from the trust view. Thus, the number of optimal teams is equivalent to the number of clusters generated by dual-view spectral clustering.

Specifically, we build teams based on standard spectral clustering in the willingness and trust networks, respectively. At the same time, consensus and similarity constraints are introduced to constrain the CCS team recruitment optimization results. The optimization function of building teams with high mutual willingness in the willingness network is as follows:

$$\min \, tr\left(\mathbf{M}^{w^\top} \mathbf{L}^w \mathbf{M}^w\right) s.t. \, \mathbf{M}^{w^\top} \mathbf{M}^w = \mathbf{I}. \tag{20}$$

Similarly, the objective function of building teams with high mutual trust in the trust network is as follows:

$$\min \, tr\left(\mathbf{M}^{t^\top} \mathbf{L}^t \mathbf{M}^t\right) s.t. \, \mathbf{M}^{t^\top} \mathbf{M}^t = \mathbf{I}, \tag{21}$$

where $\mathbf{L}^w = \mathbf{I} - (\mathbf{D}_m^w)^{-1/2} \mathbf{R}_m^w (\mathbf{D}_m^w)^{-1/2}$ and $\mathbf{L}^t = \mathbf{I} - (\mathbf{D}_m^t)^{-1/2} \mathbf{R}_m^t (\mathbf{D}_m^t)^{-1/2}$ represent the normalized Laplace matrices on the willingness and trust networks, respectively, and $\mathbf{D}_m^w$ and $\mathbf{D}_m^t$ are the diagonal degree matrices on $\mathbf{R}_m^w$ and $\mathbf{R}_m^t$.

Combining equations (14), (19–21), we finally obtain the objective function of CCS team recruitment optimization, which is formulated as follows:

$$\min \, F\left(\mathbf{M}^w, \mathbf{M}^t\right) = \min \, tr\left(\mathbf{M}^{w^\top} \mathbf{L}^w \mathbf{M}^w\right)$$

$$+ tr\left(\mathbf{M}^{t^\top} \mathbf{L}^t \mathbf{M}^t\right) + \frac{\lambda_1}{2} \mathrm{Con}\left(\mathbf{M}^w, \mathbf{M}^t\right) + \frac{\lambda_2}{2} \mathrm{Sim}\left(\mathbf{M}^w, \mathbf{M}^t\right), \tag{22}$$

$$s.t. \quad \mathbf{M}^{w^\top} \mathbf{M}^w = \mathbf{I}, \mathbf{M}^{t^\top} \mathbf{M}^t = \mathbf{I},$$

where λ_1 and λ_2 control the weights of consensus and similarity constraints, respectively.

We convert the consensus constraint term of equation (22) into the trance-norm form:

$$\frac{1}{C^2} tr\left(\mathbf{M}^w \mathbf{M}^{w^\top} \mathbf{M}^w \mathbf{M}^{w^\top} - 2\mathbf{M}^w \mathbf{M}^{w^\top} \mathbf{M}^t \mathbf{M}^{t^\top} + \mathbf{M}^t \mathbf{M}^{t^\top} \mathbf{M}^t \mathbf{M}^{t^\top}\right)$$

$$= \frac{2}{C} - \frac{2}{C^2} tr\left(\mathbf{M}^w \mathbf{M}^{w^\top} \mathbf{M}^t \mathbf{M}^{t^\top}\right). \tag{23}$$

Similarly, we transform the similarity constraint term as follows:

$$tr\left(\mathbf{M}^{t^\top} \mathbf{Z}^t \mathbf{M}^t\right) + tr\left(\mathbf{M}^{w^\top} \mathbf{Z}^w \mathbf{M}^w\right) - 2tr\left(\mathbf{M}^{t^\top} \mathbf{Z}^{w,t} \mathbf{M}^w\right), \tag{24}$$

where $\mathbf{Z}^t = \sum_{i=1}^{N} \mathbf{X}_i^t \mathbf{E} \mathbf{X}_i^{t^\top}$, $\mathbf{Z}^w = \sum_{i=1}^{N} \mathbf{X}_i^w \mathbf{E} \mathbf{X}_i^{w^\top}$, and $\mathbf{Z}^{w,t} = \sum_{i=1}^{N} \mathbf{X}_i^t \mathbf{E} \mathbf{X}_i^{w^\top}$. $\mathbf{E}$ is an all-one matrix. Ignoring the constant terms, the objective function is rewritten as follows:

$$\min \, F\left(\mathbf{M}^w, \mathbf{M}^t\right) = \min \, tr\left(\mathbf{M}^{w^\top} \widetilde{\mathbf{L}}^w \mathbf{M}^w\right)$$

$$+ tr\left(\mathbf{M}^{t^\top} \widetilde{\mathbf{L}}^t \mathbf{M}^t\right) - \lambda_1 tr\left(\mathbf{M}^w \mathbf{M}^{w^\top} \mathbf{M}^t \mathbf{M}^{t^\top}\right) - \lambda_2 tr\left(\mathbf{M}^{t^\top} \mathbf{Z}^{w,t} \mathbf{M}^w\right), \tag{25}$$

$$s.t. \quad \mathbf{M}^{w^\top} \mathbf{M}^w = I, \mathbf{M}^{t^\top} \mathbf{M}^t = I,$$

where $\widetilde{\mathbf{L}}^t = \mathbf{L}^t + (\lambda_2/2)\mathbf{Z}^t$ and $\widetilde{\mathbf{L}}^w = \mathbf{L}^w + (\lambda_2/2)\mathbf{Z}^w$.

The curvilinear search method (CSM) [46] uses an update scheme similar to Crank–Nicolson, which can retain constraints for updating with a low iterative cost. Inspired by this, to obtain the optimal solution of equation (25), we combine this constraint-keeping update method with an alternative optimization strategy [47]. Specifically, given initial $\mathbf{M}_{(0)}^t$, we alternate by optimizing one variable in each iteration while maintaining the other variable until convergence as follows:

$$\mathbf{M}_{(a+1)}^w = \arg \min_{\mathbf{M}^w} F\left(\mathbf{M}^w, \mathbf{M}_{(a)}^t\right),$$

$$s.t. \, \mathbf{M}^{w^\top} \mathbf{M}^w = \mathbf{I}, \tag{26}$$

$$\mathbf{M}_{(a+1)}^t = \arg \min_{\mathbf{M}^t} F\left(\mathbf{M}_{(a+1)}^w, \mathbf{M}^t\right),$$

$$s.t. \, \mathbf{M}^{t^\top} \mathbf{M}^t = \mathbf{I}, \tag{27}$$

where a is the number of iterations.

Based on the team assignment matrices $\mathbf{M}^w$ and $\mathbf{M}^t$ obtained from the above optimization, we fuse them to calculate the final unified team assignment matrix as follows:

$$\widetilde{\mathbf{M}} = \frac{\widetilde{\mathbf{M}}^w + \widetilde{\mathbf{M}}^t}{2}, \tag{28}$$

where

$$
\begin{aligned}
\widetilde{\mathbf{M}}^w &= \left(\mathbf{M}^w \odot \mathbf{M}^w\right)\left(\left(\mathbf{M}^w \odot \mathbf{M}^w\right)^{\top}\left(\mathbf{M}^w \odot \mathbf{M}^w\right)\right)^{-1}, \\
\widetilde{\mathbf{M}}^t &= \left(\mathbf{M}^t \odot \mathbf{M}^t\right)\left(\left(\mathbf{M}^t \odot \mathbf{M}^t\right)^{\top}\left(\mathbf{M}^t \odot \mathbf{M}^t\right)\right)^{-1}.
\end{aligned}
\tag{29}
$$

The elements of matrices $\widetilde{\mathbf{M}}^w$ and $\widetilde{\mathbf{M}}^t$ are the probability that the i th participant is assigned to the c th team in the willingness and trust networks, respectively. The matrix $\widetilde{\mathbf{M}}$ reflects the final probability distribution for all teams. Thus, we can recruit each participant to the team with the highest probability according to the matrix $\widetilde{\mathbf{M}}$. Finally, we can obtain the optimal teams recruited for CCS.

The specific process of the CCS team recruitment optimization solution is shown in Algorithm 1. The inputs of Algorithm 1 are N participants with the mutual willingness matrix R_m^w and the mutual trust matrix R_m^t, the number of recruited teams C, consensus constraint weight λ_1, similarity constraint weight λ_2, the number of neighbors K for each participant, and the maximum number of iterations Maxite. The output is the result Team $= \{\text{Team}_1, \ldots, \text{Team}_C\}$ of the recruited C teams. First, the team assignment matrices $\mathbf{M}_{(0)}^w$ and $\mathbf{M}_{(0)}^w$ are initialized. Then, CSM is used to alternately optimize $\mathbf{M}_{(a)}^w$ and $\mathbf{M}_{(a)}^w$ in each iteration until convergence. Finally, $\widetilde{\mathbf{M}}$ is calculated according to equation (28) to obtain the optimal teams recruited by CCS. The time complexity of Algorithm 1 depends mainly on the number of iterations of CSM executed in its loop body (steps 3-4). Referring to literature [46], we know that the time complexity of CSM in each iteration depends mainly on the inverse computation with complexity $O(N^3)$ in the Crank–Nicolson-like scheme. Therefore, it can be inferred that the overall time complexity of Algorithm 1 is $O(N^3)$.

5. Experiments and Analysis

In this section, we introduce the setup of the recruitment simulation platform for CCS. Then, we simulate the recruitment process using this platform and analyze the experimental results. All reported results are obtained on a machine with a 3.3 GHz Intel Core 2 Duo CPU and 2 GB RAM.

5.1. The Setup of the CCS Recruitment Simulation Platform. In this subsection, first, the QoS metric is proposed to evaluate the performance of CCS services. Second, we deploy other recruitment methods to prove the effectiveness of the proposed methods. Finally, we also present other settings for the experiments.

5.1.1. QoS Evaluation Metric for CCS Services

(1) The Impact of Mutual Willingness and Trust on Collaboration. We comprehensively consider the mutual willingness and trust relationships among participants. If mutual willingness/trust exceeds the willingness/trust threshold, it is a high willingness/trust relationship. On the contrary, it is a low willingness/trust relationship. Based on the level of mutual willingness and trust relationships between participants, the relationship between participant pairs in CCS is divided into four types: high willingness-trust, low willingness-high trust, high willingness-low trust, and low willingness-trust. A low willingness-trust relationship will lead to noncooperation among participants, which is a "malicious" relationship for CCS.

A high level of mutual willingness and trust will lead to more active collaboration. As shown in equations (30) and (31), we use an exponential function to quantify the impact of mutual willingness and trust on collaboration among participants, respectively. When mutual willingness and trust are greater than the willingness threshold and trust threshold, the impact of mutual willingness and mutual trust on collaboration among participants is greater than 1. Equation (32) calculates the degree of collaboration between participants. The higher the value, the higher the degree of collaboration between participants. A value greater than 1 indicates active collaboration, while a value less than 1 indicates negative collaboration:

$$C_{(i,j)}^w = \exp\left(-\left(\theta^w - r_m^w(i,j)\right)\right), \tag{30}$$

$$C_{(i,j)}^t = \exp\left(-\left(\theta^t - r_m^t(i,j)\right)\right), \tag{31}$$

$$C_{(i,j)} = \mu^w C_{(i,j)}^w + \mu^t C_{(i,j)}^t, \tag{32}$$

where $\mu_w, \mu_t \in [0,1]$ represent the weights of trust and willingness, respectively, and θ^w and θ^t represent the willingness and trust threshold required for the team, respectively. θ^w and θ^t are assumed to follow a normal distribution $N(\mu, \sigma^2)$, and their values are in $[0,1]$. To unify the magnitude, the value of $C_{(i,j)}$ is normalized to a value between 0 and 1.

To evaluate the performance of CCS services, we draw on the QoS evaluation model proposed by Truong et al. [48]. However, they only consider the quality of data provided by individuals and ignore the quality of collaboration in their QoS evaluation. Therefore, their metric is unsuitable for the QoS evaluation of CCS services. For this reason, we redefine the QoS evaluation metric for CCS services as follows:

$$\text{QoS}(R) = \frac{T}{\left|\log\left(\prod_{t=1}^{T} Q_{\text{Task}_t}\right)\right|}, \tag{33}$$

$$Q_{\text{Task}_t} = \frac{(1 - \alpha_{col}) \sum_{i \in \text{Team}_c} Q_i^D + \alpha_{col} Q_{\text{Team}_c}^C}{|\text{Team}_c|}, \tag{34}$$

Require: N, R_m^w, R_m^t, C, λ_1, λ_2, K, and *Maxite*
Ensure: Team $= \{$Team$_1, \cdots,$ Team$_C\}$
   (1) Initialize the team assignment matrices $\mathbf{M}_{(0)}^w$ and $\mathbf{M}_{(0)}^t$;
   (2) $a = 0$;
   (3) According to equation (26), update $\mathbf{M}_{(a)}^w$ by using CSM;
   (4) According to equation (27), update $\mathbf{M}_{(a)}^t$ by using CSM;
   (5) $a \leftarrow a + 1$;
   (6) Repeat steps 3–5 until $a =$ Maxite;
   (7) Return $\mathbf{M}^w \leftarrow \mathbf{M}_{(a)}^w$ and $\mathbf{M}^t \leftarrow \mathbf{M}_{(a)}^t$;
   (8) Calculate $\bar{\mathbf{M}}$ according to equation (28) to obtain the optimal teams Team $= \{$Team$_1, \ldots,$ Team$_C\}$ for CCS;

ALGORITHM 1: CCS team recruitment optimization solution.

$$Q_{\text{Team}_c}^C = \frac{1}{2} \sum_{i \in \text{Team}_c} \sum_{j \in \text{Team}_t \wedge i \neq j} C_{(i,j)}. \tag{35}$$

Each request R has T tasks. There is a positive correlation between the quality of service $\text{QoS}(R)$ of the request R and the quality of each sensing task Q_{Task_t}. We use the product of the natural logarithm of each task quality Q_{Task_t} to express the quality of service $\text{QoS}(R)$, as shown in equation (33). Each task is completed by a team Team$_c$. The quality of each task Q_{Task_t} is calculated by the average of data quality Q^D and team collaboration quality $Q_{\text{Team}_c}^C$, where $\alpha_{\text{col}} \in [0, 1]$ denotes the task collaboration requirement and controls their weighting. As shown in equation (35), the team collaboration quality of Team$_c$ depends on the degree of collaboration among team members.

5.1.2. Other Recruitment Method Deployment.

To verify the effectiveness of the proposed method, we set up three other recruitment methods: (1) trust-based recruitment method, (2) average-based recruitment method, and (3) random recruitment method. Unlike the versions of these methods in literature [48], which focus on individual recruitment, we adapt these methods for team recruitment in the CCS scenario. In the trust-based recruitment method, the trust between the task requester and participants is used to recruit teams, but the trust within participants is ignored. The average-based recruitment method uses average regression to predict participants' data quality scores. For better comparisons, we also set up the random recruitment method as the simplest recruitment method, which randomly selects a team from all participants. The parameter settings of these three recruitment methods are consistent with literature [48].

5.1.3. Other Settings.

The recruitment simulation platform contains multiple service requests and four team recruitment methods. The simulations of all recruitment methods have the same inputs, i.e., N participants and M service requests. After each service request, we calculate its QoS score using equations (33–35) and output it. We use grid search to set the optimal weights λ_1 and λ_2 of the consensus and similarity constraints between 10^{-1} and 10^2.

For the ranges [0.1, 1], [1, 10], and [10, 100], our steps are set to 0.1, 1, and 10, respectively. Unless otherwise specified, we set the number of participants N to 400, the number of teams C to 20, K to 5, μ_t and μ_w to 0.5, the number of platform task requests M to 160, the number of tasks per request in the range of 10 to 60, μ to 0.5, and σ to 2; the maximum number of iterations Max ite is 40 as the default value. We use the data quality Q^D score distribution of participants given in literature [48]. The high-quality participants in the platform are set to 250, and the low-quality participants are set to 150. Note that the malicious users in [48] do not belong to our research scope. We focus on the "malicious" relationship among participants.

5.2. Results and Analysis.

We evaluate the proposed method in terms of the following three aspects: First, we verify the performance of the GCN-WTN building. Second, we simulate our method in the directed small-world network (Poisson distribution) and the directed scale-free network (Power-law distribution) with different task collaboration requirements. Third, we study the effect of low willingness and trust on QoS scores. Finally, we evaluate the efficiency of the WT-TR method.

5.2.1. Performance Verification of the GCN-WTN Building.

To verify the performance of the GCN-WTN building, a willingness network of 2000 nodes and a trust network of 2000 nodes are built. We select 25239 real relationships from the Pretty Good Privacy (https://networkrepository.com/arenas%20pgp.php) dataset as the directed willingness ratings and 7988 real relationships from the Advogato (https://www.trustlet.org/datasets/advogato/) dataset as the directed trust ratings. The Pretty Good Privacy dataset is a network of cryptographic procedures, which can be seen as using the concept of "willingness" to provide encryption and authentication for data communication. The Advogato dataset is an open-source online social network where participants can authenticate one another. In the experiment, we set the convolutional layer L to 3, the learning rate to 0.005, the normalization factor λ to 10^{-5}, the initialized embedding dimension D to 128, and the number of epochs to 100. We test the prediction performance with different percentages of the training set. The prediction accuracy with the number of training epochs is shown in Figure 4.

From Figure 4, we can see that the GCN-WTN building reaches the best prediction accuracy for the willingness and trust networks in the range of 10 to 20 training epochs. For example, when the training set makes up 80% of the data, the best prediction accuracy of 0.774 is obtained at the 13th training epoch in the willingness network (as shown in Figure 4(a)). Similarly, when the training set is 80% of the data, we obtain the best prediction accuracy of 0.748 at the 13th training epoch in the trust network (as shown in Figure 4(b)). Figure 4(a) also shows that even when the training set is 30% of the total data, it achieves the best prediction accuracy of 0.748 at the 11th training epoch, which is only 0.026 lower than the value of the training set when it is 80%. In the trust network, it also achieves the best prediction accuracy of 0.702 at the 11th training epoch, a drop of 0.046 compared to the training set with 80% of the total data, as shown in Figure 4(b). This is a good indication that the GCN-WTN building is not dependent on a specific dataset and not sensitive to the size of the training set.

5.2.2. Special Cases

(1) Simulation in the Directed Small-World Network. Analysis of experimental data in literature [49] shows that many real-world networks have small-world effects. Therefore, we use a special case of the directed willingness network and directed trust networks based on a small-world network [50]. We set the number of neighbors of each node in the two networks $\langle k_w \rangle = \langle k_t \rangle = 6$, the probability of randomized reconnection $p_t = p_w = 0.1$, and the directed willingness and trust rating $r^w, r^t \in \{0.15, 0.45, 0.75, 0.95\}$, where 0.95 is the highest rating and 0.15 is the lowest rating. The proportions of these four ratings on the edge are 10%, 20%, 30%, and 40%, respectively.

The visualization of the CCS team recruitment optimization process at different time steps is shown in Figure 5. The light gray line indicates the mutual willingness relationship among participants, and the light blue line indicates the mutual trust relationship among participants. The 20 teams are represented by 20 different colors. As shown in Figure 5(a), we randomly initialize the 20 teams at $a = 0$. To evaluate the optimization performance of CCS teams at different time steps, we calculate the normalized Davies–Bouldin index (NDBI) [51] and normalized mutual information (NMI) [42] of the optimized teams in each time step, as shown in Table 1. A higher NDBI value indicates a more cohesive team. A higher NMI value indicates that the optimized teams have a higher consensus in the views of willingness and trust. From Table 1, we observe that the NDBI and NMI increase as the number of time steps increases. This means that the teams are becoming more cohesive and more consistent in their willingness and trust views. At $a = 40$, we obtain the weights λ_1 and λ_2 of consensus and similarity constraints as 4.0 and 0.7, respectively.

By simulating the four recruitment methods on the recruitment simulation platform of CCS with different task collaboration requirements, we obtain the QoS scores, as shown in Figure 6. We can see that as the task collaboration requirement α_{col} increases, the gap between the QoS scores obtained by our method and other methods keeps widening. For example, when the task collaboration requirement α_{col} of CCS is 0.5, 0.6, 0.7, 0.8, and 0.9, the gap between the average QoS score of 160 service requests of our method and the trust-based recruitment method increases from 0.3277, 1.3634, 2.5194, and 3.9197 to 5.9385. Moreover, the QoS score obtained by our method fluctuates between 8.2 and 10 when α_{col} is 0.9, as shown in Figure 6(f). It proves the advantages of the proposed method in the environment of high task collaboration requirements.

The average-based recruitment method learns from the participants' history of their previous data quality scores to select the team most likely to provide high-quality data in the next task. The trust-based recruitment method recruits the team most trusted by the task requester, which yields a slightly higher QoS score than the average-based recruitment method. This is understandable. Because trust is transitivity to a certain extent, participants recruited by the trust-based recruitment method have a certain level of trust among themselves and are more likely to cooperate. However, with the exception of our method, none of them jointly consider the willingness and trust factors that influence CCS team recruitment. This is why both the trust-based and the average-based recruitment methods obtain poor QoS scores. The teams recruited by our method comprehensively consider the willingness and trust that affect team recruitment and improve the teams' collaboration quality score. Thereby, the QoS score of CCS is improved.

(2) Simulation in the Directed Scale-Free Network. We also simulate our method in the directed scale-free network to further analyze its effectiveness. A scale-free network refers to a network whose edges obey a power-law distribution [52]; that is, very few nodes (called head nodes) have a huge number of incident edges, while most nodes (called tail nodes) have very few incident edges. We use a special case of the directed willingness network and directed trust networks based on the scale-free network. The proportion of ratings on the edge is the same as above. By simulating the four recruitment methods on the recruitment simulation platform of CCS with different task collaboration requirements, we obtain the QoS scores, as shown in Figure 7. In Figure 7, we can find that as the task collaboration requirement α_{col} increases, our method can still obtain a higher QoS score in the directed scale-free network than the other three methods. The experimental results show that the proposed method obtains the highest QoS scores in both directed small-world networks and scale-free networks, thus validating the effectiveness of our method and demonstrating its good adaptability.

5.2.3. The Influence of Low Willingness and Trust.
In addition, to explore the impact of low willingness and trust on the obtained QoS scores, we simulate the above recruitment methods when the percentage of participant pairs with a low willingness-trust relationship is different. On the basis of the
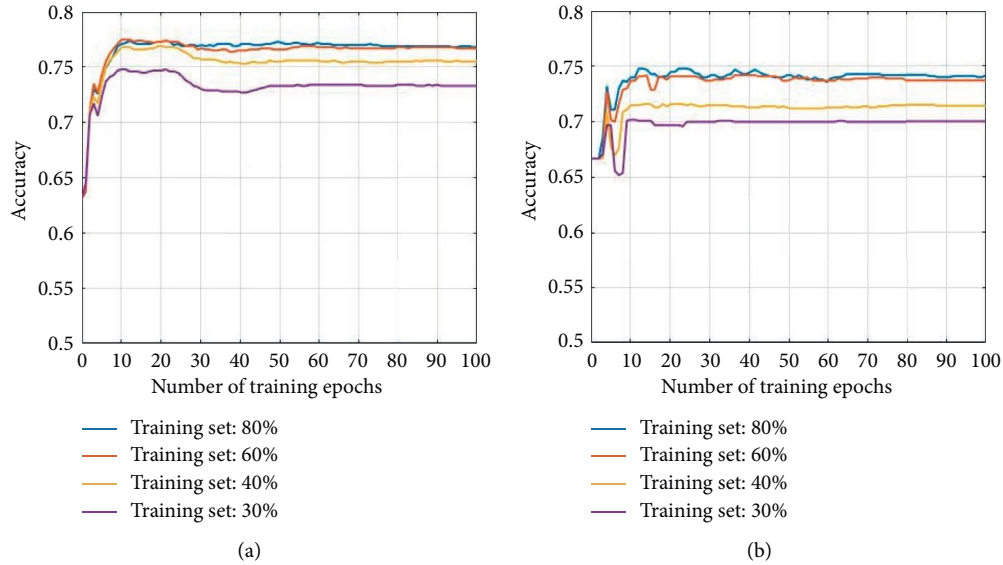
FIGURE 4: Prediction accuracy with the number of training epochs: (a) prediction accuracy in the willingness network; (b) prediction accuracy in the trust network.
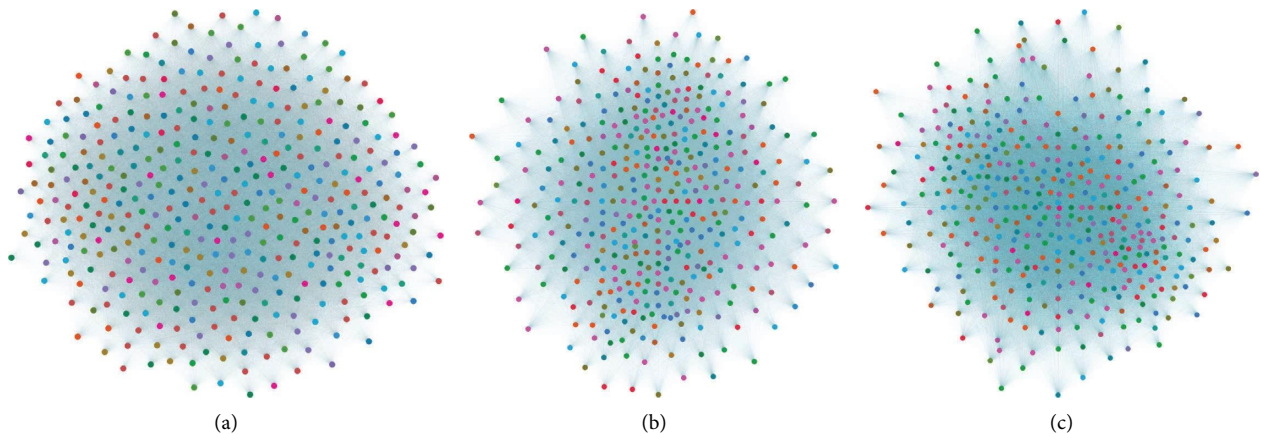

FIGURE 5: Visualization of the CCS team recruitment optimization process at different time steps: (a) $a = 0$; (b) $a = 10$; (c) $a = 40$. Nodes of the same color are recruited as a team.

TABLE 1: NDBI and NMI values at different time steps.

a	NDBI	NMI
0	0.350	0.232
10	0.475	0.430
40	0.492	0.542

experiment in the previous section, we add a low willingness-trust relationship between participant pairs that is lower than the required willingness and trust threshold. The number of teams C is set to 80, and the service request R is 50. Other settings are consistent with the above experiments. The obtained QoS scores are shown in Figures 8 and 9, where Figure 8 shows the simulation in the directed small-world network and Figure 9 shows the simulation in the directed scale-free network. The participant pairs with a low willingness-trust relationship change from 20% to 80% of the total number of participant pairs.

As shown in Figures 8 and 9, the QoS scores of all recruitment methods decrease as the percentage of participant pairs with a low willingness-trust relationship increases. This is inevitable. As the percentage of participant pairs with a low willingness-trust relationship becomes larger, the collaboration ecosystem in the recruitment simulation platform of CCS becomes progressively worse. Furthermore, as the collaboration ecosystem in the recruitment simulation platform worsens and the quality of participant collaboration decreases, the QoS score decreases. Of all the recruitment methods, our method changes most significantly as the task collaboration requirement increases. For example, in Figure 8(d), when participant pairs with a low willingness-trust relationship make up 25% of the total participant pairs, our method obtains a QoS score of 8.04. When participant pairs with a low willingness-trust relationship make up 75% of the total participant pairs, our method obtains a QoS score of 4.04. The QoS score is
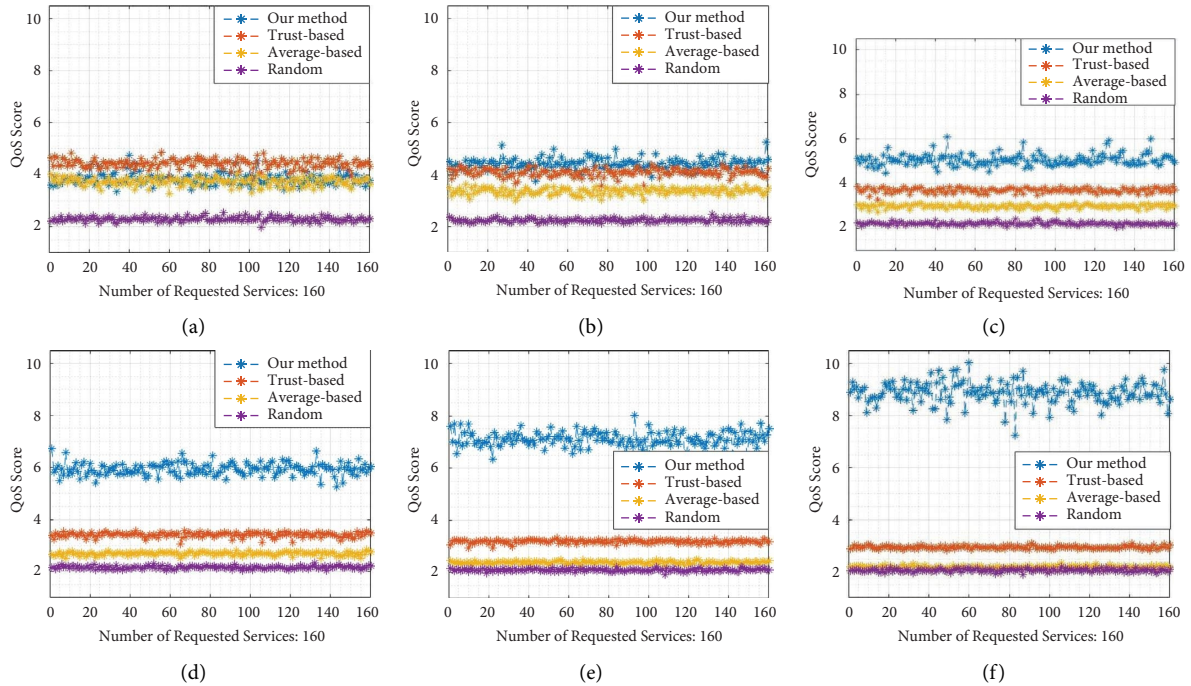
FIGURE 6: QoS scores in the directed small-world network: (a) $\alpha_{col} = 0.4$; (b) $\alpha_{col} = 0.5$; (c) $\alpha_{col} = 0.6$; (d) $\alpha_{col} = 0.7$; (e) $\alpha_{col} = 0.8$; (f) $\alpha_{col} = 0.9$.
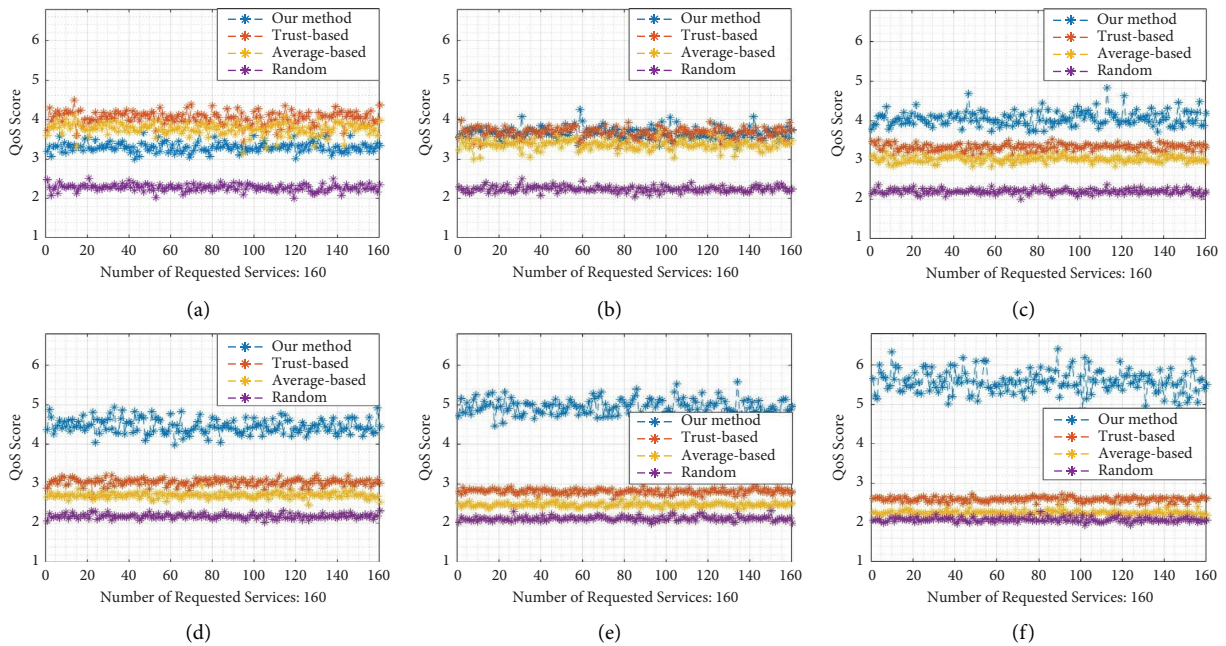

FIGURE 7: QoS scores in the directed scale-free network: (a) $\alpha_{col} = 0.4$; (b) $\alpha_{col} = 0.5$; (c) $\alpha_{col} = 0.6$; (d) $\alpha_{col} = 0.7$; (e) $\alpha_{col} = 0.8$; (f) $\alpha_{col} = 0.9$.

reduced by 4.00. This further demonstrates the high demand for CCS tasks in a cooperative ecosystem environment.

However, it is encouraging to note that the teams recruited by our method still obtain relatively higher QoS scores. This is because our method imposes consensus and similarity constraints on the willingness and trust networks. This allows participant pairs with low willingness-trust

relationships to be recruited into different teams. The degree of collaboration between participants in the same team is still greater than 1. That is, there is active collaboration. For example, when the task collaboration requirement is 0.9 and the percentage of participant pairs with a low willingness-trust relationship is 75%, our method obtains QoS scores of 4.04 and 3.05, respectively, as shown in Figures 8(d) and
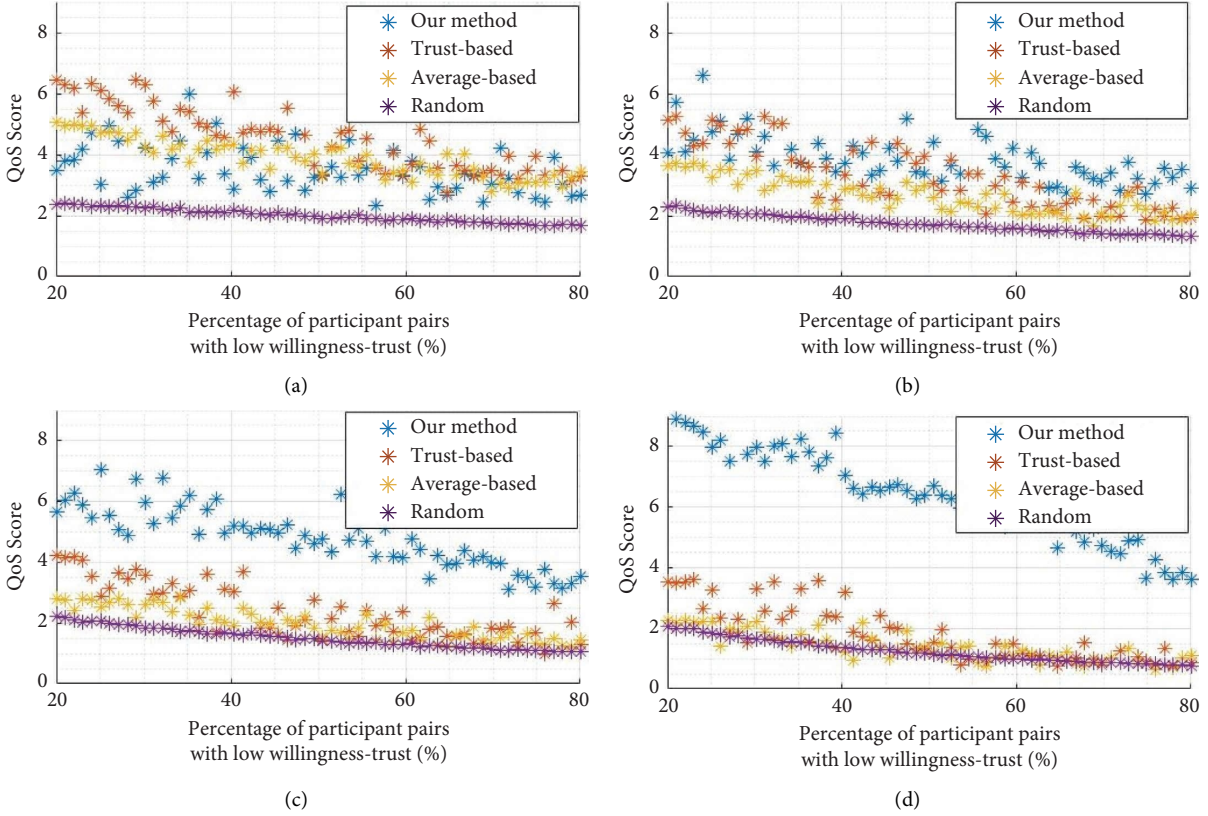
Figure 8: QoS scores with different percentages of participant pairs with low willingness-trust in the directed small-world network: (a) $\alpha_{col} = 0.3$; (b) $\alpha_{col} = 0.5$; (c) $\alpha_{col} = 0.7$; (d) $\alpha_{col} = 0.9$.
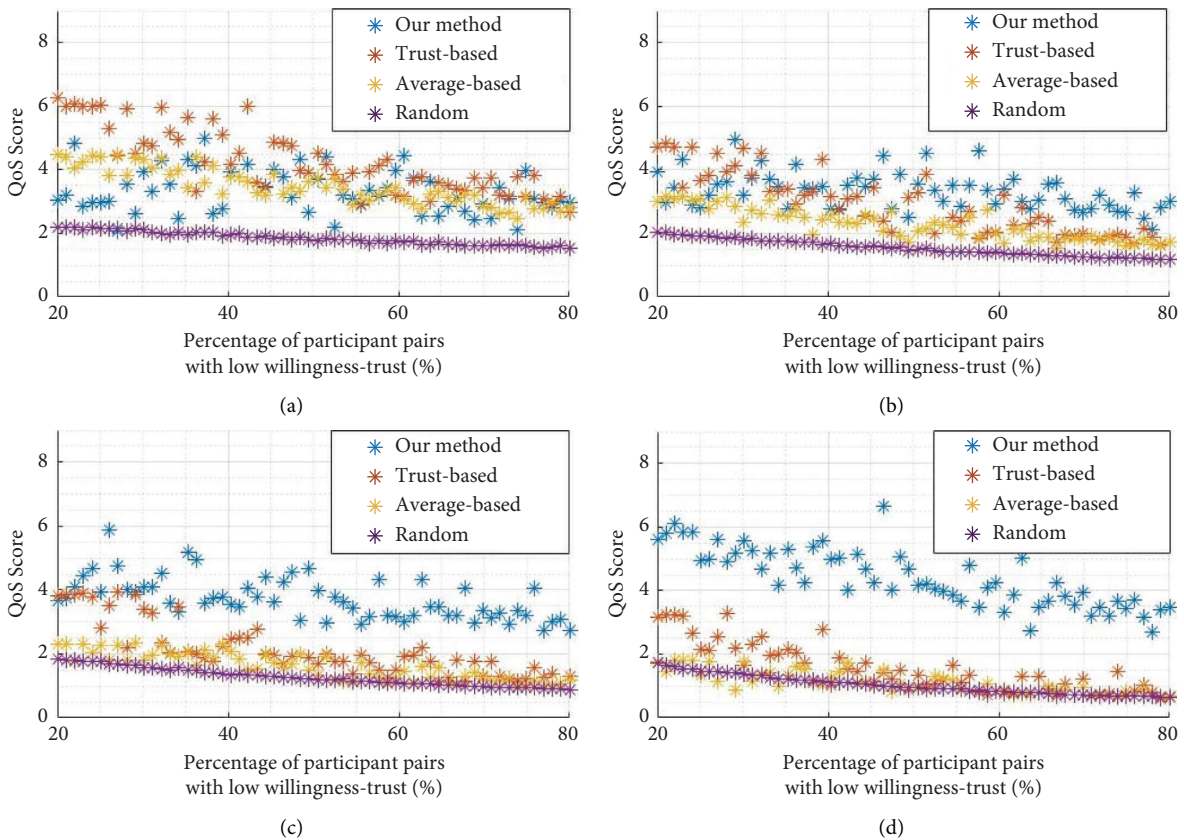

Figure 9: QoS scores with different percentages of participant pairs with low willingness-trust in the directed scale-free network: (a) $\alpha_{col} = 0.3$; (b) $\alpha_{col} = 0.5$; (c) $\alpha_{col} = 0.7$; (d) $\alpha_{col} = 0.9$.
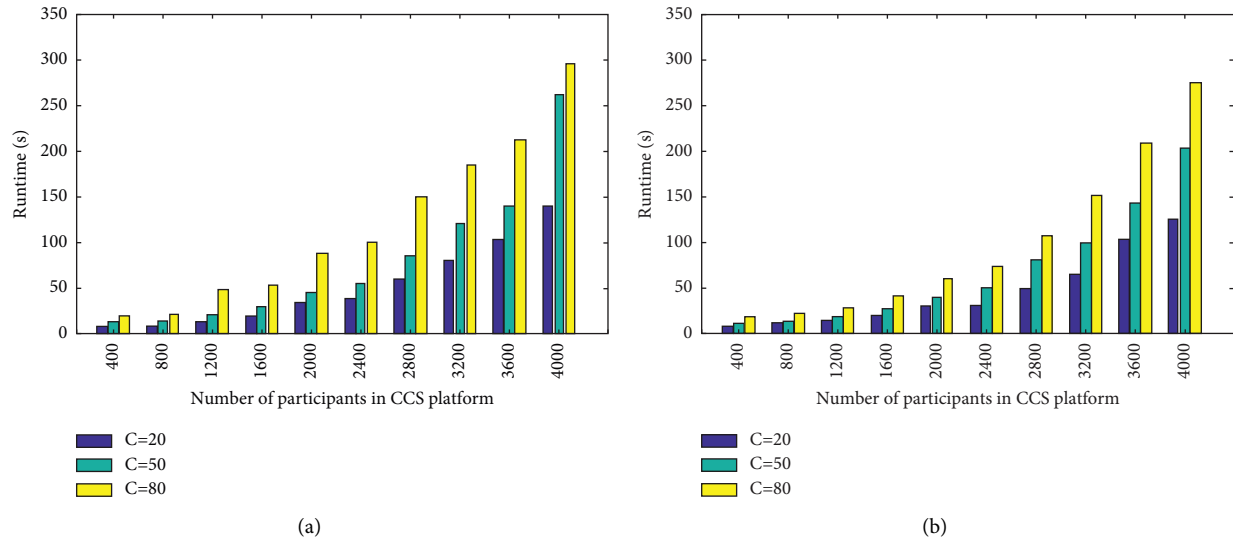
FIGURE 10: Runtime in different numbers of participants in the CCS platform: (a) runtime in the directed small-world network; (b) runtime in the directed scale-free network.

9(d). Thus, our method can still obtain a good QoS score as the percentage of participant pairs with a low willingness-trust relationship increases.

5.2.4. Efficiency of the WT-TR Method. We evaluate the efficiency of the WT-TR method by changing the size of participants in the CCS platform. Figure 10 shows the runtime of the WT-TR method in different numbers of participants in the CCS platform, where Figure 10(a) shows the runtime in the directed small-world network and Figure 10(b) shows the runtime in the directed scale-free network. The yellow bar graph demonstrates that the number of teams C is set to 80. The green bar graph demonstrates that the number of teams C is set to 50. The blue bar graph demonstrates that the number of teams C is set to 20.

As shown in Figure 10, we can see that the runtime of the WT-TR method is acceptable. In the directed small-world network with 4000 participants (as shown in Figure 10(a)), the runtime of the WT-TR method is 125.68 s for team number $C = 20$, 202.24 s for team number $C = 50$, and 275.39 s for team number $C = 80$. In a directed scale-free network with 4000 participants (as shown in Figure 10(b)), the runtime of the WT-TR method is 139.78 s for team number $C = 20$, 262.68 s for team number $C = 50$, and 295.20 s for team number $C = 80$. In practice, the number of participants in a given task area cannot be very large due to the limited population capacity of the area where the CCS task is located. Therefore, it shows that our method is efficient and capable of handling team recruitment with relatively large participant sizes in CCS platforms.

6. Conclusion and Future Work

Our study focuses on how to recruit the optimal teams for CCS so that they can collaborate mutually to complete the sensing tasks with higher QoS. To address this problem,

we design a novel team recruitment scheme for CCS that jointly considers willingness and trust. First, we build a GCN-WTN model for CCS to obtain the mutual willingness and trust among participants more accurately. Second, we propose a WT-TR method to recruit the optimal teams for CCS. This method introduces the consensus and similarity constraints into the willingness and trust networks to better meet the collaboration needs of CCS. Finally, we implement a recruitment simulation platform for CCS to simulate the team recruitment process and validate the effectiveness of our proposed method. The experimental results show that the teams recruited by the proposed method can significantly improve QoS for CCS.

We provide an outlook for future research from the following aspects. First, the proposed method does not limit the recruitment cost or the number of participants. It will be our future work to further consider them based on the proposed method. Second, as group roles are important factors in improving team performance, we plan to combine GRA with our WT-TR model to recruit more competitive teams in the future. Third, considering the variability of participants across willingness and trust networks, the similarity between different teams would be more helpful to recruit the optimal teams for CCS [53]. Fourth, it is also a problem worth exploring to promote the collaboration of participants in CCS by integrating other mechanisms, such as incentive mechanisms.

Data Availability

The datasets generated and/or analyzed during the current study are available from the corresponding author upon reasonable request.

Conflicts of Interest

The authors declare that they have no conflicts of interest.

Acknowledgments

References

[1] B. Guo, Z. Wang, Z. Yu et al., "Mobile crowd sensing and computing: the review of an emerging human-powered sensing paradigm," *ACM Computing Surveys*, vol. 48, no. 1, pp. 1–31, 2015.

[2] G. Zhang, D. Lu, and H. Liu, "IoT-based positive emotional contagion for crowd evacuation," *IEEE Internet of Things Journal*, vol. 8, no. 2, pp. 1057–1070, 2021.

[3] Y. Gao, X. Li, J. Li, and Y. Gao, "A dynamic-trust-based recruitment framework for mobile crowd sensing," in *Proceedings of the of IEEE International Conference on Communications (ICC)*, pp. 1–6, Paris, France, May 2017.

[4] J. Wang, F. Wang, Y. Wang, D. Zhang, L. Wang, and Z. Qiu, "Social-network-assisted worker recruitment in mobile crowd sensing," *IEEE Transactions on Mobile Computing*, vol. 18, no. 7, pp. 1661–1673, 2019.

[5] A. Hamrouni, H. Ghazzai, M. Frikha, and Y. Massoud, "A spatial mobile crowdsourcing framework for event reporting," *IEEE Transactions on Computational Social Systems*, vol. 7, no. 2, pp. 477–491, 2020.

[6] A. Singla, E. Horvitz, P. Kohli, and A. Krause, "Learning to hire teams," in *Proceedings of the Of AAAI Conference on Human Computation and Crowdsourcing (HCOMP)*, pp. 1–10, Palo Alto, CA, USA, November 2015.

[7] Q. Liu, T. Luo, R. Tang, and S. Bressan, "An efficient and truthful pricing mechanism for team formation in crowdsourcing markets," in *Proceedings of the IEEE International Conference on Communications (ICC)*, pp. 567–572, Seoul, Korea, January 2015.

[8] H. Jiang and S. Matsubara, "Efficient task decomposition in crowdsourcing," in *Proceedings of the. Of International Conference on Principles and Practice of Multi-Agent Systems (PRIMA)*, pp. 65–73, Cham, Switzerland, November 2014.

[9] I. Lykourentzou, A. Antoniou, and Y. Naudet, "Matching or crashing? Personality-Based team formation in crowdsourcing environments," *Computer Science*, vol. 2, no. 1, pp. 1–14, 2015.

[10] J. M. Flores-Parra, M. Castañón-Puga, R. D. Evans, R. Rosales-Cisneros, and C. Gaxiola-Pacheco, "Towards team formation using belbin role types and a social networks analysis approach," in *Proceedings of the of IEEE Technology and Engineering Management Conference (TEMSCON)*, pp. 1–6, Evanston, IL, USA, June 2018.

[11] G. Awal and K. Bharadwaj, "Team formation in social networks based on collective intelligence–an evolutionary approach," *Applied Intelligence*, vol. 41, no. 2, pp. 627–648, 2014.

[12] R. Azzam, R. Mizouni, H. Otrok, A. Ouali, and S. Singh, "GRS: a group-based recruitment system for mobile crowd sensing," *Journal of Network and Computer Applications & Computer Applications*, vol. 72, pp. 38–50, 2016.

[13] K. Isomura, *Organization Theory by chester barnard: An Introduction*, Springer, Singapore, 2020.

[14] P. Lencioni, *The Five Dysfunctions of a Team: A Leadership Fable*, Jossey-Bass, San Francisco, CA, USA, 2012.

[15] S. Yang, M. Barlow, K. Kasmarik, and E. Lakshika, "A novel trust architecture integrating differentiated trust and response strategies for a team of agents," *International Journal of Intelligent Systems*, vol. 36, no. 12, pp. 7017–7052, 2021.

[16] A. Taghavi, E. Eslami, E. Herrera-Viedma, and R. Ureña, "Trust based group decision making in environments with extreme uncertainty," *Knowledge-Based Systems*, vol. 191, Article ID 105168, 2020.

[17] O. Ayadi, N. Halouani, and F. Masmoudi, "A fuzzy collaborative assessment methodology for partner trust evaluation," *International Journal of Intelligent Systems*, vol. 31, no. 5, pp. 488–501, 2016.

[18] K. Dirks, "The effects of interpersonal trust on work group performance," *Journal of Applied Psychology*, vol. 84, no. 3, pp. 445–455, 1999.

[19] F. Zhang, B. Jin, H. Liu, Y. W. Leung, and X. Chu, "Minimum-cost recruitment of mobile crowdsensing in cellular networks," in *Proceedings of the of IEEE Global Communications Conference (GLOBECOM)*, pp. 1–7, Washington, DC, USA, December 2016.

[20] Y. Hu, J. Wang, B. Wu, and S. Helal, "Participants selection for from-scratch mobile crowdsensing via reinforcement learning," in *Proceedings of the of IEEE International Conference on Pervasive Computing and Communications (PerCom)*, pp. 1–10, Austin, TX, USA, March 2020.

[21] H. Gao, Y. Xiao, H. Yan, Y. Tian, D. Wang, and W. Wang, "A Learning-based credible participant recruitment strategy for mobile crowd sensing," *IEEE Internet of Things Journal*, vol. 7, no. 6, pp. 5302–5314, 2020.

[22] Z. Wang, J. Zhao, J. Hu et al., "Towards personalized task-oriented worker recruitment in mobile crowdsensing," *IEEE Transactions on Mobile Computing*, vol. 20, no. 5, pp. 2080–2093, 2021.

[23] K. Ota, M. Dong, J. Gui, and A. Liu, "QUOIN: incentive mechanisms for crowd sensing networks," *IEEE Network*, vol. 32, no. 2, pp. 114–119, 2018.

[24] H. Jin, B. He, L. Su, K. Nahrstedt, and X. Wang, "Data-driven pricing for sensing effort elicitation in mobile crowd sensing systems," *IEEE/ACM Transactions on Networking*, vol. 27, no. 6, pp. 2208–2221, 2019.

[25] C. Lv, T. Wang, C. Wang, F. Chen, and C. Zhao, "ESPPTD: an efficient slicing-based privacy-preserving truth discovery in mobile crowd sensing," *Knowledge-Based Systems*, vol. 229, no. 8, p. 2021, Article ID 107349, 2021.

[26] F. Restuccia, P. Ferraro, T. S. Sanders, S. Silvestri, S. K. Das, and G. L. Re, "FIRST: a framework for optimizing information quality in mobile crowdsensing systems," *ACM Transactions on Sensor Networks*, vol. 15, no. 1, pp. 1–35, 2018.

[27] T. Wolf, A. Schröter, D. Damian, L. D. Panjer, and T. H. Nguyen, "Mining task-based social networks to explore collaboration in software teams," *IEEE Software*, vol. 26, no. 1, pp. 58–66, 2009.

[28] A. Hamrouni, H. Ghazzai, T. Alelyani, and Y. Massoud, "Optimal team recruitment strategies for collaborative mobile crowdsourcing systems," in *Proceedings of the of IEEE Technology & Engineering Management Conference (TEMSCON)*, pp. 1–6, Novi, MI, USA, June 2020.

[29] R. Azzam, R. Mizouni, H. Otrok, S. Singh, and A. Ouali, "A stability-based group recruitment system for continuous

mobile crowd sensing," *Computer Communications*, vol. 119, pp. 1–14, 2018.

[30] E. Wang, Y. Yang, J. Wu, W. Liu, and X. Wang, "An efficient prediction-based user recruitment for mobile crowdsensing," *IEEE Transactions on Mobile Computing*, vol. 17, no. 1, pp. 16–28, 2018.

[31] H. Zhu, "Predict team performance with E-CARGO," in *Proceedings of the Of IEEE International Conference on Systems, Man, and Cybernetics (SMC)*, pp. 3559–3564, Miyazaki, Japan, January 2018.

[32] Q. Jiang, H. Zhu, Y. Qiao, D. Liu, and B. Huang, "Extending group role assignment with cooperation and conflict factors via KD45 logic," *IEEE Transactions on Computational Social Systems*, vol. 10, no. 1, pp. 178–191, 2023.

[33] H. Zhu and Y. Zhu, "Group role assignment with agents' busyness degrees," in *Proceedings of the Of IEEE International Conference on Systems, Man, and Cybernetics (SMC)*, pp. 3201–3206, Banff, Canada, October 2017.

[34] H. Zhu, "Group multi-role assignment with conflicting roles and agents," *IEEE/CAA Journal of Automatica Sinica*, vol. 7, no. 6, pp. 1498–1510, 2020.

[35] R. Cheng and M. Xiao, "Greedy task assignment algorithm for collaborative crowdsensing," *Journal of Chinese Computer Systems*, vol. 38, no. 5, pp. 1039–1043, 2017.

[36] Y. Xu, Z. Gong, J. Y. Forrest, and E. Herrera-Viedma, "Trust propagation and trust network evaluation in social networks based on uncertainty theory," *Knowledge-Based Systems*, vol. 234, Article ID 107610, 2021.

[37] S. Lu, Z. Zhu, J. M. Gorriz, S. H. Wang, and Y. D. Zhang, "NAGNN: classification of COVID-19 based on neighboring aware representation from deep graph neural network," *International Journal of Intelligent Systems*, vol. 37, no. 2, pp. 1572–1598, 2022.

[38] S. Fu, W. Liu, K. Zhang, Y. Zhou, and D. Tao, "Semi-supervised classification by graph p-laplacian convolutional networks," *Information Sciences*, vol. 560, pp. 92–106, 2021.

[39] W. S. A. W. Ahlim, N. H. Kamis, S. A. S. Ahmad, and F. Chiclana, "Similarity–trust network for clustering-based consensus group decision-making model," *International Journal of Intelligent Systems*, vol. 37, no. 4, pp. 2758–2773, 2022.

[40] D. Zhang, L. Yao, K. Chen, S. Wang, X. Chang, and Y. Liu, "Making sense of spatio-temporal preserving representations for EEG-based human intention recognition," *IEEE Transactions on Cybernetics*, vol. 50, no. 7, pp. 3033–3044, 2020.

[41] Y. Gui, D. Li, and R. Fang, "A fast adaptive algorithm for training deep neural networks," *Applied Intelligence*, vol. 53, no. 4, pp. 4099–4108, 2023.

[42] A. Kumar, P. Rai, and H. Daumé, "Co-regularized multi-view spectral clustering," in *Proceedings of the Of International Conference on Neural Information Processing Systems (NIPS)*, pp. 1413–1421, Granada, Spain, December 2011.

[43] L. Nie, X. Song, and T. Chua, "Learning from multiple social networks," *Synthesis Lectures on Information Concepts Retrieval and Services*, vol. 8, no. 2, pp. 1–118, 2016.

[44] L. Fu, P. Lin, A. V. Vasilakos, and S. Wang, "An overview of recent multi-view clustering," *Neurocomputing*, vol. 402, pp. 148–161, 2020.

[45] H. Lian, H. Xu, S. Wang, M. Li, X. Zhu, and X. liu, "Partial multiview clustering with locality graph regularization," *International Journal of Intelligent Systems*, vol. 36, no. 6, pp. 2991–3010, 2021.

[46] Z. Wen and W. Yin, "A feasible method for optimization with orthogonality constraints," *Mathematical Programming*, vol. 142, no. 1-2, pp. 397–434, 2013.

[47] M. Luo, X. Chang, L. Nie, Y. Yang, A. G. Hauptmann, and Q. Zheng, "An adaptive semisupervised feature analysis for video semantic recognition," *IEEE Transactions on Cybernetics*, vol. 48, no. 2, pp. 648–660, 2018.

[48] N. B. Truong, G. M. Lee, T. W. Um, and M. Mackay, "Trust evaluation mechanism for user recruitment in mobile crowdsensing in the internet of things," *IEEE Transactions on Information Forensics and Security*, vol. 14, no. 10, pp. 2705–2719, 2019.

[49] C. Korte and S. Milgram, "Acquaintance networks between racial groups: application of the small world method," *Journal of Personality and Social Psychology*, vol. 15, no. 2, pp. 101–108, 1970.

[50] D. Watts and S. Strogatz, "Collective dynamics of 'small-world' networks," *Nature*, vol. 393, no. 6684, pp. 440–442, 1998.

[51] U. Maulik and S. Bandyopadhyay, "Performance evaluation of some clustering algorithms and validity indices," *IEEE Transactions on Pattern Analysis and Machine Intelligence*, vol. 24, no. 12, pp. 1650–1654, 2002.

[52] A. Barabási and E. Bonabeau, "Scale-free networks," *Scientific American*, vol. 288, no. 5, pp. 60–69, 2003.

[53] K. Chen, L. Yao, D. Zhang, X. Wang, X. Chang, and F. Nie, "A Semisupervised recurrent convolutional attention model for human activity recognition," *IEEE Transactions on Neural Networks and Learning Systems*, vol. 31, no. 5, pp. 1747–1756, 2020.